Evaluation of Atypical Cytochrome P450 Kinetics with Two-Substrate Models: Evidence That Multiple Substrates Can Simultaneously Bind to Cytochrome P450 Active Sites†

K. R. Korzekwa,*,‡ N. Krishnamachary,‡ M. Shou,§ A. Ogai,‡ R. A. Parise,‡ A. E. Rettie,|| F. J. Gonzalez,⊥ and T. S. Tracy#

Center for Clinical Pharmacology, University of Pittsburgh, Pittsburgh, Pennsylvania 15217, Department of Drug Metabolism, Merck Research Laboratories, West Point, Pennsylvania 19486, Department of Medicinal Chemistry, University of Washington, Seattle, Washington 98195, Laboratory of Metabolism, National Cancer Institute, National Institutes of Health, Bethesda, Maryland 20892, and Department of Basic Pharmaceutical Sciences, School of Pharmacy, West Virginia University, Morgantown, West Virginia 26506

Received June 30, 1997; Revised Manuscript Received January 9, 1998

ABSTRACT: Some cytochrome P450 catalyzed reactions show atypical kinetics, and these kinetic processes can be grouped into five categories: activation, autoactivation, partial inhibition, substrate inhibition, and biphasic saturation curves. A two-site model in which the enzyme can bind two substrate molecules simultaneously is presented which can be used to describe all of these observed kinetic properties. Sigmoidal kinetic characteristics were observed for carbamazepine metabolism by CYP3A4 and naphthalene metabolism by CYPs 2B6, 2C8, 2C9, and 3A5 as well as dapsone metabolism by CYP2C9. Naphthalene metabolism by CYP3A4 and naproxen metabolism by CYP2C9 demonstrated nonhyperbolic enzyme kinetics suggestive of a low K_m, low V_{max} component for the first substrate molecule and a high K_m, high V_{max} component for the second substrate molecule. 7,8-Benzoflavone activation of phenanthrene metabolism by CYP3A4 and dapsone activation of flurbiprofen and naproxen metabolism by CYP2C9 were also observed. Furthermore, partial inhibition of 7,8-benzoflavone metabolism by phenanthrene was observed. These results demonstrate that various P450 isoforms may exhibit atypical enzyme kinetics depending on the substrate(s) employed and that these results may be explained by a model which includes simultaneous binding of two substrate molecules in the active site.

The cytochrome P450 enzymes are the most important enzymes in the metabolism of hydrophobic drugs, carcinogens, and other foreign compounds. In the area of drug metabolism, there is a significant effort to predict in vivo pharmacokinetic and pharmacodynamic characteristics from in vitro data. If valid, these in vitro−in vivo correlations can be used to predict pharmacokinetic properties and the potential for drug interactions, as well as the genotypic and phenotypic variabilities in the population. An essential component of a useful in vitro−in vivo correlation is the saturation profile of a drug.

Most P450[1] oxidations show hyperbolic saturation kinetics and competitive inhibition between substrates. Therefore, some pharmacokinetic properties can be predicted with standard Michaelis−Menten kinetic analyses; e.g., drug interactions can be predicted from inhibition studies. However, some P450 reactions show unusual enzyme kinetics, and most of these identified so far are associated with oxidations by the CYP3A P450s. The unusual kinetic characteristics of the CYP3A enzymes (and less frequently other enzymes) include four categories: activation, autoactivation, partial inhibition, and substrate inhibition. Activation is an increased reaction velocity in the presence of another compound. The compound 7,8-benzoflavone was first shown to activate dexamethasone-induced microsomal catalysis, and, later, catalysis by purified CYP3A enzymes (Wrighton et al., 1986; Schwab et al., 1988). Autoactivation occurs when the activator is the substrate itself, resulting in sigmoidal saturation kinetics. Johnson and co-workers (Johnson et al., 1988; Schwab et al., 1988) reported that the metabolism of progesterone by CYP3A6 yields nonlinear Lineweaver−Burke kinetics. The kinetics reverted to linearity by the addition of 5 μM 7,8-benzoflavone (Schwab et al., 1988). Similar results were recently reported for several other CYP3A reactions (Ueng et al., 1997). For partial inhibition, saturating concentrations of the inhibitor do not completely inhibit substrate metabolism. Substrate inhibition occurs when an increase in substrate concentration beyond a certain value results in a decrease in the rate of metabolism.

† Supported by NSF Grant OSR-9450578 and NIH Grants NO1-DK-6-2274 and GM32165.

* To whom correspondence should be addressed at the Center for Clinical Pharmacology, 623 Scaife Hall, University of Pittsburgh Medical Center, Pittsburgh, PA 15213.

‡ University of Pittsburgh.

§ Merck Research Laboratories.

|| University of Washington.

⊥ National Cancer Institute.

West Virginia University.

[1] Abbreviations: P450, cytochrome P450; CYP, cytochrome P450; *m*-dapsone, 3-aminophenyl sulfone; NSAID, nonsteroidal antiinflammatory drug; [E_t], total enzyme concentration; HPLC, high-pressure liquid chromatography; PAH, polycyclic aromatic hydrocarbon; BaP, benzo[*a*]pyrene.

S0006-2960(97)01562-6 CCC: $15.00
Published on Web 03/03/1998

In this report, we describe an additional saturation profile that is biphasic in nature. This profile occurs when an enzyme has both a low K_m−low V_{max} component and a high K_m−high V_{max} component. Although the resulting curve is similar to that observed for a two-enzyme model, it is one of the expected profiles for a single enzyme with two binding sites.

The central hypothesis of this report is that the most atypical kinetics are due to the simultaneous binding of more than one substrate to an enzyme's active site. The active site is defined as the region in the interior of the protein from which a substrate has access to the active oxygen. Although it has been recently suggested (Ueng et al., 1997) that these interactions are due to allosteric binding at two distinct sites, previous studies in our laboratory suggest that activation of phenanthrene metabolism by 7,8-benzoflavone involves the simultaneous binding of both 7,8-benzoflavone and the other substrate in the same active site. We will show that all observed kinetic properties can be described by a two-substrate model. Although the kinetic models described do not differentiate between two substrates which bind in the same active site or two independent sites, these two possibilities can be evaluated from the predicted topology of the cytochrome P450 enzymes and the simultaneous metabolism of two different substrates.

EXPERIMENTAL PROCEDURES

Chemicals. Carbamazepine, naphthalene, 1-naphthol, 2-naphthol, 7,8-benzoflavone, dapsone, and *m*-dapsone were purchased from Aldrich Chemical Co. (Milwaukee, WI). Flurbiprofen, 4′-hydroxyflurbiprofen, and 2-fluoro-4-biphenylacetic acid were gifts from Upjohn Co. (Kalamazoo, MI). Naproxen and desmethylnaproxen were gifts from Syntex Co. (Palo Alto, CA). *N*-Hydroxydapsone was a gift from James Porter, University of Pittsburgh. All other chemicals were reagent grade.

Enzyme Preparations. Construction of the recombinant vaccinia virus vectors containing the cDNAs encoding the P450 proteins has been reported previously (Gonzalez et al., 1991). Cells were harvested 24 h after infection with the appropriate recombinant vaccinia virus. For the control experiments, HepG2 cells were infected with the wild-type virus. The P450 contents were determined by Fe^{2+}-CO versus Fe^{2+} difference spectroscopy, and protein concentrations are determined by standard methods (Omura & Sato, 1964). For the metabolism studies, the cells were lysed by sonication and centrifuged at 500000*g* for 10 min. The membrane pellets were resuspended with a Teflon/glass homogenizer.

Construction of baculovirus vectors for expressing CYP2C9 and subsequent purification of the recombinant enzyme have been reported previously (Haining et al., 1996). Purified enzymes were reconstituted in dilaurylphosphatidylcholine vesicles (extruded through a 200 nm pore size membrane) along with P450 reductase and cytochrome b_5, in a ratio of 1:2:1.

Carbamazepine 10,11-Oxide Formation. Carbamazepine was incubated at 37 °C with 25 pmol of expressed CYP3A4 in 1 mL of 50 mM potassium phosphate, with 1 mM NADPH for 20 min. Substrate comsumption was less than 10%. The reaction was stopped with 2 mL of dichloromethane, and 2-naphthol was added as an internal standard. Carbamazepine, carbamazepine 10,11-epoxide, and internal standard were separated with a Thomson 20/20 C18 column (2.5 mm i.d. × 20 cm; 5 μm particle size). Analytes were eluted with the following methanol/water gradients at 1 mL/min: 5 min at 50:50, followed by a linear gradient to 60:40 over 35 min, followed by a linear gradient to 70:30 over 10 min, and finally a linear gradient to 100:0 over 10 min. Substrate, metabolite, and internal standard were detected at 210 nm with a UV detector, and quantitated by relating peak areas to a standard curve.

4′-Hydroxyflurbiprofen Formation. Human liver microsomes or purified recombinant CYP2C9 enzyme were incubated with 1−150 μM *(S)*-flurbiprofen and 0−25 μM dapsone in 100 mM potassium phosphate buffer (pH 7.4) and NADPH and reacted for 20 min at 37 °C. The samples were quenched with 500 μL of acetonitrile containing 9 ng of 2-fluoro-4-biphenylacetic acid (internal standard), acidified with 20 μL of H_3PO_4, and 300 μL of H_2O was added. The samples were centrifuged at 10 000 rpm for 4 min, and the supernate was transferred to a clean tube. To the supernate was added 2 mL of ethyl acetate; samples were vortexed for 1 min and then centrifuged at 3000 rpm for 5 min. The upper organic layer was removed and evaporated to dryness. Following reconstitution in 150 μL of mobile phase, 10−50 μL was analyzed by HPLC for the formation of 4′-hydroxyflurbiprofen as described previously (Tracy et al., 1996). For the lowest concentrations of flurbiprofen, substrate consumption was as high as 30%. Therefore, substrate concentrations were corrected with the integrated Michaelis−Menten equation: $S' = (S_0 - S)/[\ln (S_0/S)]$. The difference between parameter estimates for the corrected and uncorrected analyses was less than 5%, and the fits were equivalent.

Desmethylnaproxen Formation. The formation of desmethylnaproxen from naproxen was measured according to the methods of Tracy et al. (1997). Incubations were carried out exactly as described for flurbiprofen. Substrate consumption was less than 10% for all incubations. Incubations were quenched by adding 200 μL of acetonitrile containing 480 ng of 2-fluoro-4-biphenylacetic acid (internal standard) followed by 20 μL of H_3PO_4. The samples were vortexed at 10 000 rpm for 4 min, and 5−22 μL was directly injected on the HPLC column. The mobile phase consisted of (30:70) acetonitrile/20 mM K_2HPO_4, pH 3, pumped at 1 mL/min through a Brownlee Spheri-5 C_{18} 4.6 × 100 mm column. Analytes were detected by determining the fluorescence at an excitation wavelength of 230 nm and an emission wavelength of 340 nm.

Dapsone Metabolism. Metabolism of dapsone to the *N*-hydroxy metabolite was determined with vaccinia-expressed CYP2C9. Incubations contained 30 pmol of CYP2C9, 0−500 μM dapsone, and 1 mM NADPH in 50 mM potassium phosphate buffer, pH 7.4. Reactions were incubated for 20 min at 37 °C and stopped by the addition of 2 mL of dichloromethane and internal standard (5 μg of *m*-dapsone). Substrate consumption was less than 10% for all incubations. The reactions were extracted, and the organic phase was evaporated under nitrogen. The samples were then dissolved in 250 μL of aqueous HPLC buffer. Metabolites were separated on a Thomson 20/20 ODS column with a gradient of 0:100 to 50:50 (acetonitrile + 0.05%

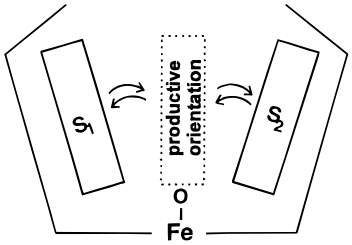

FIGURE 1: Simple scheme for two substrates in a P450 active site. Both substrates have access to productive orientations through translations and rotations.

trifluoroacetic acid)/(10 mM heptanesulfonic acid + 0.05% trifluoroacetic acid) over 20 min. Metabolites were quantitated by the UV absorbance at 317 nm. Retention times were 13.9 for *N*-hydroxydapsone, 15.1 for dapsone, and 16.0 for *m*-dapsone.

Naphthalene Metabolism. Metabolism of naphthalene to 1-naphthol was determined with vaccinia-expressed P450 enzymes. Incubations contained expressed enzyme, the appropriate amount of naphthalene, and 1 mM NADPH in 50 mM phosphate buffer, pH 7.4. Reactions were incubated for 20 min at 37 °C and stopped by the addition of 1.5 mL of pentane and internal standard (β-naphthol). Substrate consumption was less than 10% for all incubations. The reactions were extracted and centrifuged at 5000 rpm for 5 min. The incubations were placed on dry ice until the aqueous phase was frozen. The pentane layer was immediately decanted into concentration tubes, and 30 μL of *n*-propanol was added. The pentane was carefully removed under nitrogen, leaving the *n*-propanol. Then 100 μL of water was added and injected directly on the HPLC. Metabolites were separated on a Thomson 20/20 ODS column with a gradient of 35:65 to 70:30 acetonitrile/water over 15 min. Metabolites were quantitated by the UV absorbance at 254 nm. Retention times for the internal standard and 1-naphthol were 13.9 and 14.4 min, respectively.

Kinetic Derivations and Analyses. Symbolic determinants were constructed according to the method of King and Altman (1956). Symbolic determinants were solved, and the resulting equations were simplified using the program Mathematica (Wolfram Research, Champain, IL). Two-dimensional and surface plots of equations were prepared and statistics of the fits were determined using Axum 5.0 (Mathsoft, Inc.).

RESULTS

Kinetic Models. The hypothesis we are investigating is that two substrates can bind simultaneously within the active site of a P450 enzyme. Therefore, the following kinetic equations were derived for an enzyme with two binding sites. Although the two substrates must occupy different regions at any one time, we are proposing that both substrates have access to the reactive oxygen, as shown in Figure 1. Although two different substrate molecules are likely to have preferred orientations within the active site, for simplicity, our derivations will not distinguish between these orientations (i.e., $ES_1S_2 \equiv ES_2S_1$). These equations are applicable to any two-site model, including models that have distinct allosteric binding sites. Using available symbolic math computer programs, rate equations can be generated for almost any kinetic scheme. However, many of the resulting equations are complex and cannot be simplified into forms that can be interpreted easily. In these cases, the rapid equilibrium assumption can be used to derive manageable equations. The rapid equilibrium models assume that the interchange between species is rapid, relative to the catalytic steps in the model. Although this assumption may not be valid for the P450 enzymes, the resulting forms of the equations may be similar to the correct equations. An example of this is provided in the first derivation below. In the following section, derivations are provided for some single-substrate and two-substrate models.

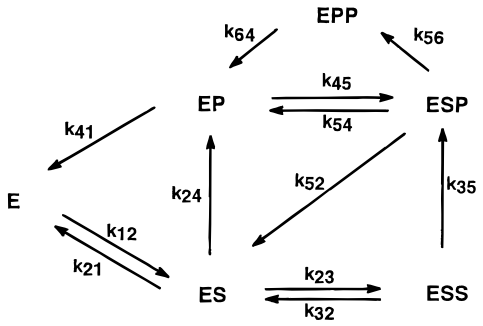

FIGURE 2: Proposed kinetic scheme for an enzyme with two binding sites within an active site and a single substrate component.

One Substrate−Two Binding Sites. The kinetic scheme for an enzyme with two binding sites and a single substrate is given in Figure 2. In this model, product can be formed either from the single substrate-bound form, ES, or from the two-substrate-bound form, ESS. Although the full rate equation is very complex, if product release is fast relative to the oxidation rates, the velocity equation is simplified to equation 1:

$$\frac{v}{[E_t]} = \frac{k_{24}([S]/K_{m1}) + k_{35}([S]^2/K_{m1}K_{m2})}{1 + [S]/K_{m1} + [S]^2/K_{m1}K_{m2}} \quad (1)$$

In this equation, $K_{m1} = (k_{21} + k_{24})/k_{12}$ and $K_{m2} = (k_{23} + k_{35})/k_{32}$. This equation was derived using the method of King and Altman (1956). The symbolic determinants were solved and the resulting equations simplified using Mathematica. This is an exact solution to the model in Figure 2. An equation of the same form is obtained if the rapid equilibrium assumption is used, except equilibrium constants replace the K_m constants, e.g., $K_{s1} = k_{21}/k_{12}$.

This equation is relatively simple, consisting of four relevant constants. K_{m1} would be the standard Michaelis constant for the binding of the first substrate, if [ESS] = 0. K_{m2} would be the standard Michaelis constant for the binding of the second substrate, if [E] = 0 (i.e., the first binding site is saturated). In the complete equation, these constants are not true K_m values, but their form [i.e., $K_{m1} = (k_{21} + k_{24})/k_{12}$] and significance are analogous. Likewise, k_{24} and k_{35} are $V_{max}/[E_t]$ terms when the enzyme is saturated with one and two substrate molecules, respectively. Although this equation is relatively simple, several different saturation profiles can be obtained. Since the conditions responsible for some of the saturation profiles may not be intuitive, we have provided the examples in Figure 3.

Panel A shows that if the two K_m and V_{max} terms are similar, the resulting saturation curve is very close to

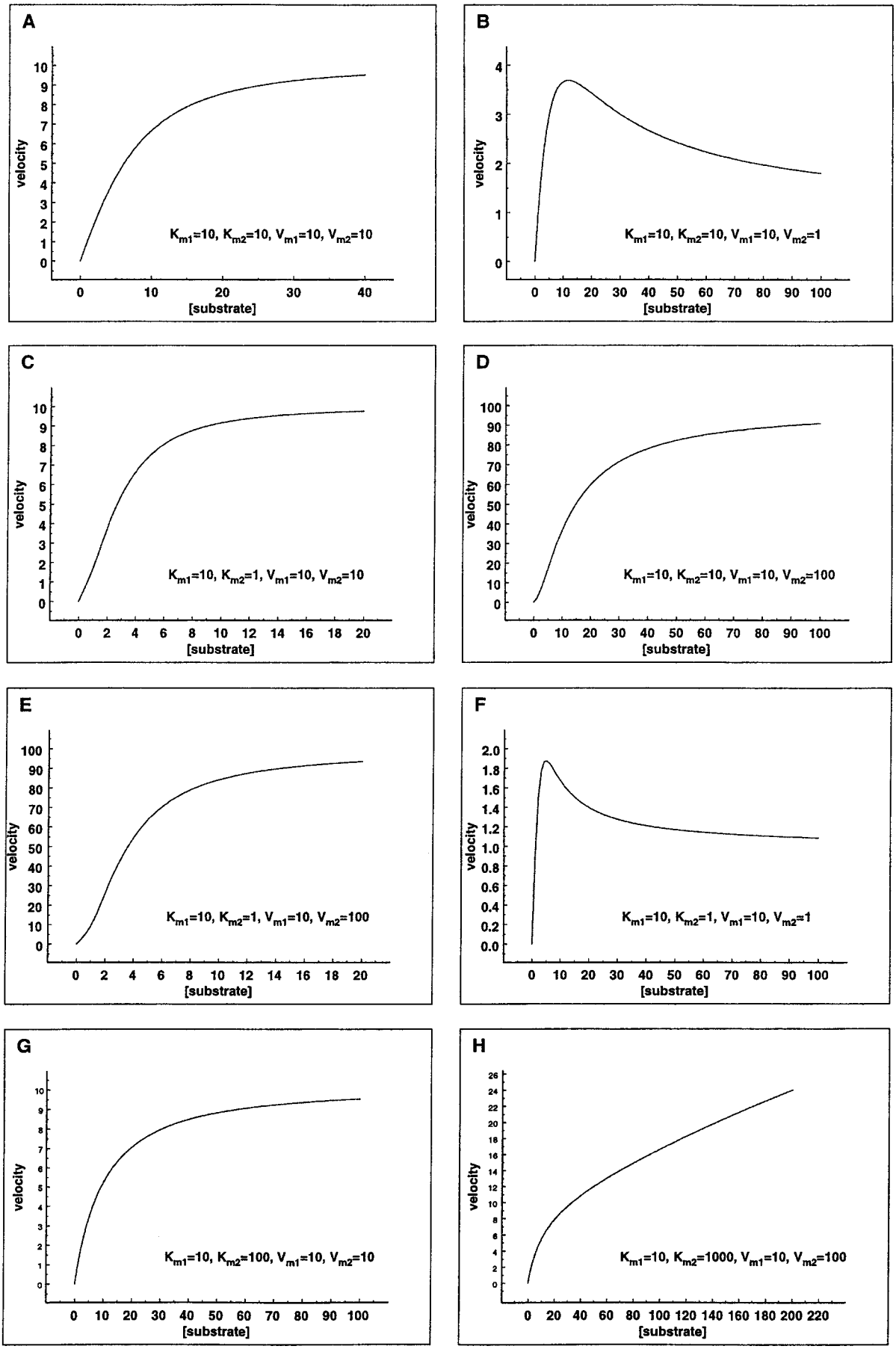

FIGURE 3: Theoretical saturation profiles for an enzyme with two substrate binding sites representing various kinetics and eq 1. Panels represent kinetic parameters given in each respective panel.

hyperbolic. For example, a fit of the curve in Figure 3A to a hyperbola gives the following values: $K_m = 7.9$, $V_{max} = 11.7$, and $R^2 = 0.994$. Therefore, under these conditions, a two-site model is likely to be experimentally indistinguishable from a single-site model.

Figure 3B shows the saturation curve observed when $V_{max2} < V_{max1}$ and $K_{m2} = K_{m1}$. When V_{max2} is substantially lower than V_{max1}, substrate inhibition is evident. If the second binding site is a saturable site, the velocity will plateau at V_{max2} at high substrate concentrations [hyperbolic inhibition (Cleland, 1979)]. Again, this profile does not define the mechanism of interaction or the nature of the second binding site. For example, if high concentrations of substrate interfere with electron transfer from the reductase to the P450, substrate inhibition would be observed. In addition, moderate changes in V_{max} upon binding of the second substrate may be difficult to detect. For example, if both V_{max2} and K_{m2} are moderately smaller than V_{max1} and K_{m1}, the curve will appear hyperbolic.

Panels C−E of Figure 3 show sigmoidal saturation curves. The curve in Figure 3C is obtained when $K_{m2} < K_{m1}$ and $V_{max1} = V_{max2}$. This is essentially a result of a sigmoidal *binding* curve for the enzyme, in which the singly bound substrate increases the affinity of the enzyme for the second substrate molecule. However, for enzymatic systems, a change in binding characteristics is not required for a sigmoidal concentration−velocity curve. Figure 3D shows the saturation profile observed when $K_{m1} = K_{m2}$ and $V_{max2} > V_{max1}$. In this case, a very similar sigmoidal saturation curve is obtained without a change in the binding constant of the enzyme. The sigmoidal characteristic is due to an increase in V_{max} for the ESS complex. Figure 3E shows the sigmoidal plot obtained when both $K_{m2} < K_{m1}$ and $V_{max2} > V_{max1}$. Since V_{max1} cannot be independently determined, it is not possible to determine whether sigmoidal kinetics are due to increased binding affinity of ES or increased velocity from ESS or both. All three models fit well to the Hill equation.

Figure 3F shows the saturation profile observed when both $K_{m2} < K_{m1}$ and $V_{max2} < V_{max1}$. Again, substrate inhibition is observed. Compared with Figure 3B, less of V_{max1} is manifest since the second substrate binds with high affinity to ES. As $K_{m2} \ll K_{m1}$, the velocity contribution of ES is negligible, and the saturation curve appears to be hyperbolic with kinetic constants of K_{m2} and V_{max2} (plot not shown).

Figure 3G ($V_{max2} = V_{max1}$ and $K_{m2} > K_{m1}$) shows an essentially hyperbolic plot. Whereas Figure 3A is very close to hyperbolic, Figure 3F demonstrates that the influence of a second binding site disappears as its K_m gets larger. In fact, the fit of Figure 3G to a hyperbola gives $K_m = 10.0$, $V_{max} = 10.5$, and $R^2 = 0.9996$.

Finally, Figure 3H shows a biphasic saturation profile in which $V_{max2} > V_{max1}$ and $K_{m2} \gg K_{m1}$. At higher substrate concentrations, the velocity approaches V_{max2}. This profile looks similar to that for a mixture of two different enzymes, one saturating at low concentrations, and one with a very high K_m. When $K_{m2} > K_{m1}$ and $V_{max2} > V_{max1}$, the saturation curves for a two-site model also fit a two-enzyme model, over the entire relevant concentration range. When $[S] \ll K_{m2}$ and $K_{m2} \gg K_{m1}$, the two-enzyme model can be described by eq 2, whereas the appropriate equation for the two-site model is given in eq 3:

$$v = \frac{V_{max1}[S]}{K_{m1} + [S]} + \frac{V_{max2}}{K_{m2}}[S] \quad (2)$$

$$v = \frac{V_{max1}[S] + (V_{max2}/K_{m2})[S]^2}{K_{m1} + [S]} \quad (3)$$

Although both equations provide good fits to this model, the values of the constants estimated from the equations can vary dramatically when [S] approaches K_{m2}.

The above section (1) provides examples of the types of kinetic profiles that can be seen for an enzyme that can bind two substrate molecules and (2) describes the limitations that are inherent in interpreting any experimental data. Two kinetic profiles can readily be associated with a two-site model: substrate inhibition and a sigmoidal saturation curve. However, the nature of the binding sites and the values of the kinetic constants may be difficult to determine. For example, a sigmoidal concentration curve could be due to a decrease in K_m for the second substrate or an increase in V_{max} from the ESS complex. Whereas an exceptional data set may converge to the appropriate model, moderate experimental error will result in either large standard errors for the parameter estimates or multiple solutions of the least-squares regression analyses with eq 1.

Two Substrates−Two Binding Sites. The complete scheme for two different substrates that can bind to two sites on an enzyme is complex, with six different enzyme species (Figure 4). Since the kinetic equations associated with this model cannot be easily interpreted, simplifying assumptions are made. A model that we make extensive use of is shown in Figure 5. In this model, two different molecules can bind to the enzyme, but the metabolism of only one substrate is considered. For this scheme, S is the substrate, and B is an effector. Formation of the effector metabolites from EB and ESB is not included in the kinetic derivations. If B is also metabolized, the rate constants k_{42} and k_{31} will be composites of both debinding and metabolism of the effector molecule. Again, we make the assumption that product release is fast. Although the rate equation has been derived, it cannot be easily simplified. Therefore, we use equations based on the rapid equilibrium assumption. Rapid equilibrium equations can be readily derived, and the substrate−effector model has been discussed previously (Segel, 1975). One form of the velocity equation is given in eq 4:

$$v = V_{max}[S]/\{K_m[(1 + [B]/K_B)/(1 + \beta[B]/\alpha K_B)] + [S][(1 + [B]/\alpha K_B)/(1 + [B]/\alpha K_B)]\} \quad (4)$$

In this equation, S is the substrate and B is the effector, $V_{max} = k_{25}[Et]$, $K_m = (k_{21} + k_{25})/k_{12}$ (kinetic constants for substrate metabolism), $K_B = k_{31}/k_{13}$ (binding constant for effector), α is the change in K_m resulting from effector binding, and β is the change in V_{max} from effector binding. For inhibitors, $\beta < 1$, and for activators, $\beta > 1$.

Although eq 4 is derived with the rapid equilibrium assumption, it may be valid for P450 enzymology for the following reasons. First, the rapid equilibrium assumption for the model in Figure 2 has the same form as the complete steady-state equation. Second, eq 4 can provide very good fits to experimental data (see below).

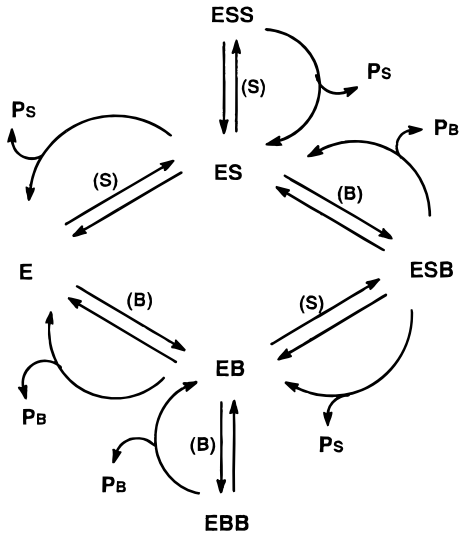

FIGURE 4: Proposed kinetic scheme for an enzyme with two binding sites within the active site and two distinct substrates. The scheme shows all possible enzyme species.

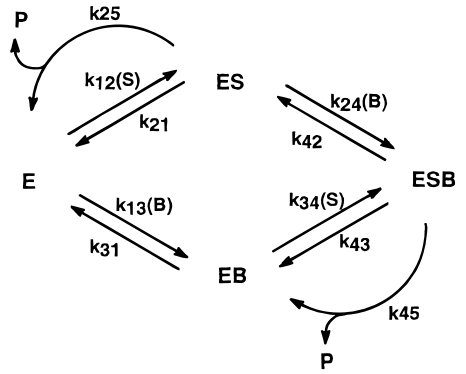

FIGURE 5: Simplified kinetic scheme for the interaction between a substrate and an effector molecule for an enzyme with two binding sites within the active site.

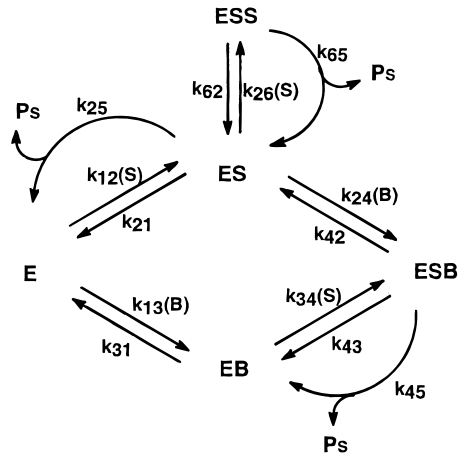

FIGURE 6: Kinetic scheme for an enzyme with two binding sites that can bind two substrate molecules and one effector molecule.

Although equations for more complex models may be difficult to interpret, they can be used to evaluate potential kinetic characteristics. As an example, consider the kinetic scheme in Figure 6. In this scheme, an effector can bind to one of two sites, and the substrate can bind to both sites. Although the rate equation is too cumbersome to be included here, it was used to predict the kinetic characteristics for the model in Figure 6. If the velocity from ESS is different

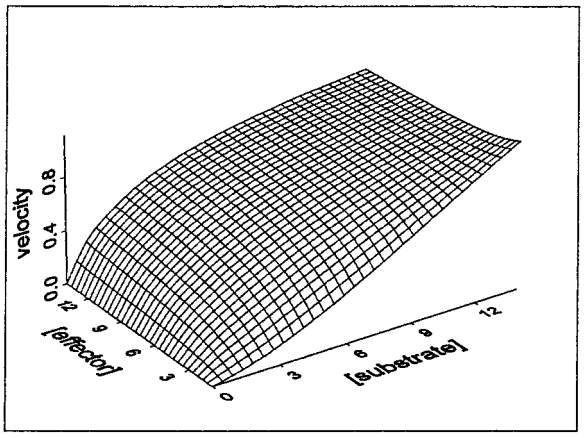

FIGURE 7: Substrate−effector saturation surface for the model in Figure 5.

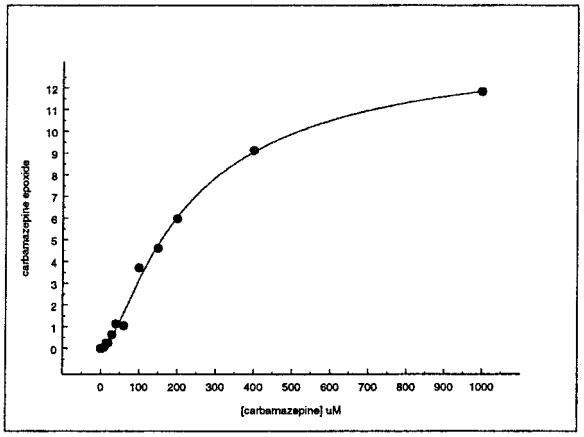

FIGURE 8: Saturation profile for carbamazepine metabolism by CYP3A4. The curve is representitive of three separate experiments.

than that for ES, then the influence of effector B can be dependent on the substrate concentration. For example, if $k_{65} > k_{45} > k_{25}$, then the effector will be an activator at low substrate concentrations (since the velocity from ESB > ES), and an inhibitor at high substrate concentrations (since the velocity from ESS > ESB). We can model this situation by assigning values to rate constants for Figure 6. Plotting the resulting velocitites, we obtain the surface shown in Figure 7. As expected, in the absence of effector, the saturation profile is sigmoidal. The effector acts as an activator at low substrate concentrations and as an inhibitor at high substrate concentrations. An example of this phenomenon has been recently reported for some CYP3A-catalyzed reactions (Ueng et al., 1997).

EXPERIMENTAL RESULTS

We will present experimental results for some cytochrome P450 enzymes that are consistent with two-site models. Although most activation and non-Michaelis−Menten kinetics have been reported for the CYP3A enzyme, we present data showing that these characteristics are possible for other P450 enzymes as well.

Carbamazepine Metabolism by CYP3A4. Carbamazepine is a classic CYP3A substrate that shows sigmoidal saturation kinetics. A saturation curve for the formation of carbamazepine 10,11-epoxide is shown in Figure 8. The result in Figure 8 is representative of three different analyses. The

Table 1: Regression Analyses for Non-Michaelis−Menten Saturation Curves

substrate	eq[a]	V_{max}[b] (SE)	V_{max2} (SE)	K_{m1}[c] (SE)	K_{m2} (SE)	K (SE)	n (SE)	(V/K)[d] (SE)	RSS[e]	R^2	F
carbamazepine	1	0.05 (1.60)	14.27 (0.96)	89 (87)	189 (57)				0.763	0.9958	476
carbamazepine	1	1.14 (1.49)	13.74 (0.40)	157 (22)	157 (22)				0.795	0.9956	684
carbamazepine	1	12.37 (0.43)	12.37 (0.43)	623 (166)	103 (51)				1.078	0.9941	504
carbamazepine	5	(0.43)	14.28 (0.75)	87 (40)	190 (47)				0.763	0.9958	713
carbamazepine	6	13.05 (0.56)				2943 (1470)	1.48 (0.11)		0.829	0.9954	656
naphthalene	3	0.10 (0.01)		17 (3)				0.834 (0.02)	4.7e-05	0.9997	4267
naphthalene	6	3.30 (7.39)				477 (880)	0.70 (0.12)		7.0e-04	0.9954	290
dapsone	1	0.02 (0.10)	0.58 (0.06)	10 (31)	110 (41)				0.00250	0.9894	93
dapsone	5		0.57 (0.05)	19 (20)	107 (38)				0.00250	0.9893	154
dapsone	5		0.52 (0.03)	63 (7)	63 (7)				0.00310	0.9867	223
dapsone	1	0.48 (0.03)	0.48 (0.03)	262 (129)	53 (48)				0.00260	0.9889	148
dapsone	1	0.22 (0.26)	0.53 (0.03)	100 (53)	100 (53)				0.00249	0.9894	155
dapsone	6	0.48 (0.04)	(0.03)			2028 (2516)	1.68 (0.30)		0.00343	0.9853	112
naproxen	1	12.03 (2.64)	50.37 (2.52)	56 (18)	1010 (237)				1.08	0.9993	2352
naproxen	3	28.23 (2.17)		184 (26)				6.62 (1.13)	3.57	0.9975	1078
naproxen	6	56.51 (3.59)				131 (12)	0.73 (0.03)		1.49	0.9990	2597

[a] V_{max} (min^{-1}). [b] The different solutions are obtained using initial parameter estimates similar to the final solutions. [c] K_m (μM). [d] $(V_{max}/K_m)_2 \times 1000$. [e] Residual sum of squares.

$$\text{eq 1: } v = \left(\frac{V_{max1}S}{K_{m1}} + \frac{V_{max2}S^2}{K_{m1}K_{m2}}\right)\Big/\left(1 + \frac{S}{K_{m1}} + \frac{S^2}{K_{m1}K_{m2}}\right) \qquad \text{eq 5: } (V_{max1} = 0)\ v = \left(\frac{V_{max2}S^2}{K_{m1}K_{m2}}\right)\Big/\left(1 + \frac{S}{K_{m1}} + \frac{S^2}{K_{m1}K_{m2}}\right)$$

$$\text{eq 3: } (K_{m2} \gg K_{m1})\ v = \left(\frac{V_{max1}S + (V/K)_2S^2}{K_{m1} + S}\right) \qquad \text{eq 6 (Hill equation): } v = \frac{V_{max1}S^n}{K + S^n}$$

results clearly show a sigmoidal saturation curve. Regression analyses result in several potential solutions, some of which are given in Table 1. A unique solution for the fit to eq 1 is not possible, due to the inherent errors in the experimental data. The different solutions are obtained using initial parameter estimates similar to the final solutions. However, analyses of the three data sets suggest the following: (1) V_{max1} ($k_{24}[E_t]$) is probably very small; i.e., ESS is probably responsible for product formation. (2) The binding constants are in the 100 μM range. (3) This results in a concave-upward region of the saturation curve in the 0−75 μM range.

Naphthalene Metabolism. Several CYPs have the capability of metabolizing polycyclic aromatic hydrocarbons (PAH). Since the active site of CYPs, such as CYP3A4, can accommodate substrates as large as dibenzopyrenes (six rings), it would not be surprising that more than one molecule of the smallest PAH, naphthalene (two rings), could fit within the confines of the active site at one time. The metabolism of naphthalene to 1-naphthol by expressed CYP3A4 exhibited non-Michaelis−Menten kinetics (Figure 9), similar to the biphasic model presented in Figure 3G with low K_m and V_{max} values for ES and high K_m and V_{max} values for ESS. The line is the least-squares fit to eq 3. The regression analyses for the fit of the data to eq 3 and the Hill equation are given in Table 1. The fit to eq 3 is significantly better than to the Hill equation. The fit to the Hill equation becomes poorer as the difference between K_{m1} and K_{m2} becomes larger.

Other CYPs, such as CYP1A1, can also accommodate substrates as large as dibenzopyrenes (six rings), and thus it is not unexpected that the metabolism of naphthalene to 1-naphthol by expressed CYP1A1 shows a sigmoidal saturation curve and that CYP2B6, CYP2C8, CYP2C9, and CYP3A5 (data not shown) also exhibit non-Michaelis−Menten kinetics. These data suggest that enzymes other than the CYP3A enzymes can have kinetic characteristics consistent with a two-site model.

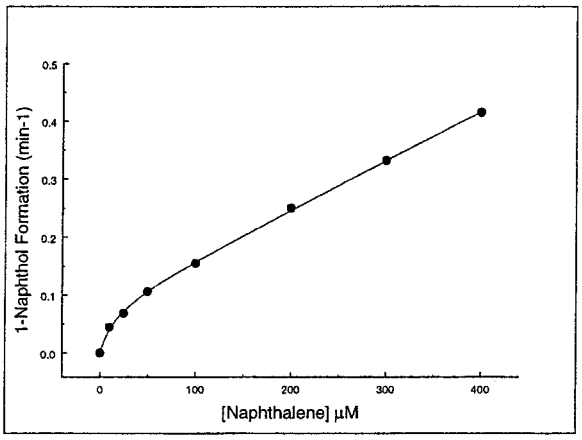

FIGURE 9: Saturation profile for CYP3A4-mediated naphthalene metabolism demonstrating nonhyperbolic kinetics. Data are the average of three experiments.

Dapsone Metabolism by CYP2C9. In results discussed below, dapsone is shown to activate NSAID metabolism by CYP2C9. As observed for 7,8-benzoflavone metabolism by CYP3A4, dapsone is also a substrate for the enzyme that it activates. The saturation profile for dapsone metabolism by expressed CYP2C9 clearly shows a sigmoidal curve (Figure 10). The results of regression analyses are given in Table 1. Although unique solutions to eq 1 are not possible for sigmoidal saturation curves, one solution gives a low K_m of 10 μM for binding of the first substrate and a higher K_m of 110 μM for binding the second. These binding constants would be consistent with the activation data presented below, in which the dapsone binding constant for CYP2C9 was found to be 17 μM. Therefore, dapsone activation may be due to the binding of a single

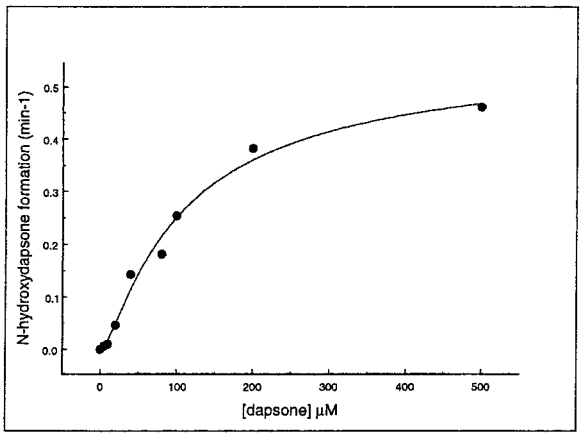

FIGURE 10: Saturation profile for CYP2C9-mediated dapsone metabolism demonstrating sigmoidal saturation kinetics.

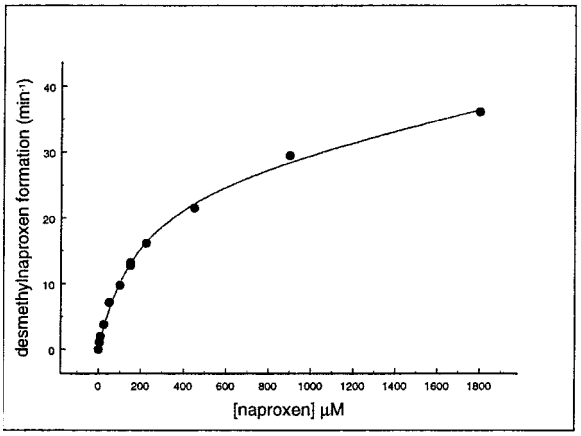

FIGURE 11: Saturation profile for CYP2C9-mediated naproxen metabolism demonstrating nonhyperbolic kinetics.

dapsone molecule to a low K_m binding region within the active site.

Naproxen Metabolism by CYP2C9. Similar to naphthalene metabolism by CYP3A4 (Figure 9), naproxen metabolism by expressed CYP2C9 appears to have a low K_m, low V_{max} component for the first substrate, and a high K_m, and high V_{max} for the second substrate (Figure 11). The curve shown is the fit to eq 1. The results of the regression analyses are given in Table 1. For this data set, the fit to eq 1 gives K_{m1} and K_{m2} values of 56 and 1010 μM, respectively. The fit to eq 3 is not as significant as the fit to eq 1, since the highest substrate concentration used approaches K_{m2}. For this data set, the fit to the Hill equation is similar to the fit to eq 1.

Metabolism of Two Different Substrates. In a previous study, the mechanism by which 7,8-benzoflavone activates CYP3A4 was studied with a series of polycyclic aromatic hydrocarbons and a series of activators and inhibitors (Shou et al., 1994a). Kinetic analyses were performed to characterize the effect of 7,8-benzoflavone on phenanthrene metabolism. It was found that 7,8-benzoflavone dramatically increases V_{max} with little effect on the K_m. This suggests that the effect is allosteric in nature, since the 7,8-benzoflavone did not displace phenanthrene from the active site. However, it was also found that 7,8-benzoflavone is also a good substrate for CYP3A4. The kinetic analysis of 7,8-benzoflavone metabolism and the effect of phenanthrene on the kinetic parameters showed that phenanthrene causes a decrease in V_{max} with no major effect on K_m.

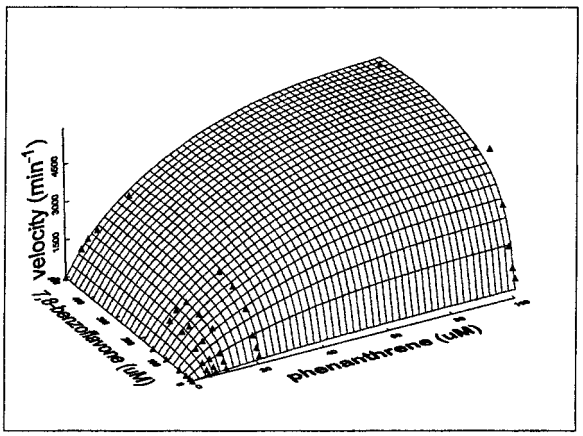

FIGURE 12: Activation of CYP3A4-mediated phenanthrene metabolism by 7,8-benzoflavone. The surface is the theoretical fit to eq 4.

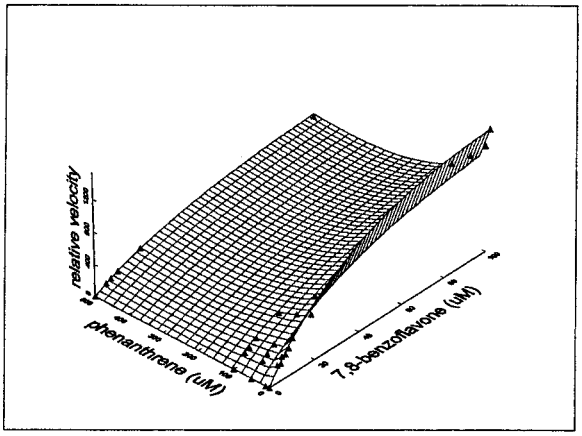

FIGURE 13: Inhibition of CYP3A4-mediated 7,8-benzoflavone metabolism by phenanthrene. The surface is the theoretical fit to eq 4.

These results provide compelling evidence that both substrates (or substrate and activator) are simultaneously present in the active site. Both compounds must have access to the active oxygen, since neither phenanthrene nor 7,8-benzoflavone can competitively inhibit each other. Increasing concentrations of a competitive inhibitor would cause the apparent K_m of the substrate to increase.

These previously reported results can be reanalyzed using the model in Figure 5 and eq 4. For the phenanthrene/7,8-benzoflavone experiments, 7,8-benzoflavone would be the effector for phenanthrene metabolism, and phenanthrene would be the effector for 7,8-benzoflavone metabolism. α is the change in K_m resulting from effector binding, and β is the change in V_{max} from effector binding. For inhibitors, $\beta < 1$, and for activators, $\beta > 1$.

The experimental data have been fit to eq 4, and the resulting surfaces are shown in Figures 12 and 13, and the resulting kinetic parameters are given in Table 2. The β values show that 7,8-benzoflavone is a strong activator of phenanthrene metabolism (15.7-fold) and phenanthrene is a partial inhibitor of 7,8-benzoflavone metabolism (maximum inhibition is 48%). The α values show that the binding constants are relatively unaffected by the presence of the other substrate (for competitive inhibitors, $\alpha \rightarrow \infty$). These data suggest that phenanthrene cannot displace 7,8-benzoflavone from the active site and vice versa.

Table 2: Kinetic Parameters for Phenanthrene/7,8-Benzoflavone Metabolism[a]

substrate	V_{max} (min^{-1})	K_m (μM)	K_B (μM)	α	β	R^2
phenanthrene	557	31	49	1.1	15.7	0.98
7,8-benzoflavone	2111	40	29	1.8	0.52	0.99

[a] The parameter estimates are the result of the fit of the data in Figure 12 to eq 4.

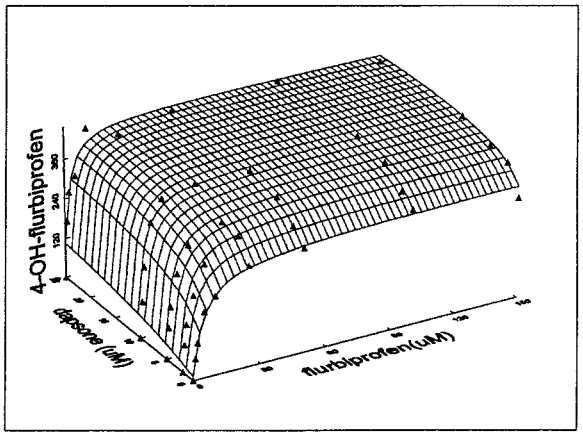

FIGURE 14: Activation of flurbiprofen metabolism by dapsone in liver microsomes. The surface is the theoretical fit to eq 4.

Table 3: Effect of Dapsone on Purified P450 2C9 Activity (Flurbiprofen Hydroxylation)

[(*S*)-flurbiprofen] (μM)	[dapsone] (μM)	4′-OH-flurbiprofen act. (min^{-1}) (SD)
10	0	0.46 (0.05)
10	10	0.94 (0.04)
10	25	0.97 (0.04)

As described previously, it appears that flurbiprofen is almost exclusively metabolized by CYP2C9 (Tracy et al., 1996). Dapsone, on the other hand, is metabolized by CYP3A4, CYP2E1, and CYP2C9 (May et al., 1992; Coleman et al., 1989) (and unpublished results with expressed enzymes). We were surprised to find that low concentrations of dapsone increased the metabolism of flurbiprofen by human liver microsomes. The saturation curves for flurbiprofen metabolism with increasing concentrations of dapsone are shown in Figure 14. The surface plots show both the experimental data and the surface for the predicted rates of metabolism based on the scheme in Figure 5, and eq 4. The resulting fit in Figure 14 gives an $R^2 = 0.985$, $V_{max} = 348$, $K_m = 4.5$ μM, $K_B = 17.7$ μM, $\alpha = 0.23$, and $\beta = 1.27$. The K_m for flurbiprofen is similar to that in the absence of dapsone. The values for α and β suggest that dapsone increases the affinity of the enzyme for flurbiprofen and activates flurbiprofen metabolism.

To assess whether this activation of flurbiprofen 4′-hydroxylation by dapsone is mediated directly through cytochrome P450 2C9, we conducted a series of experiments using purified P450 2C9 and measured whether dapsone could activate flurbiprofen metabolism in a reconstituted enzyme system. The results of these studies are presented in Table 3. These data show that low concentrations of dapsone double the rate of flurbiprofen metabolism with purified enzyme. As with the human liver microsomal data shown in Figure 14, the effect is saturated at around 10 μM dapsone.

Naproxen−Dapsone Interactions. We previously showed that CYP2C9 is the principal enzyme in human liver microsomes for the metabolism of naproxen to desmethylnaproxen (Tracy et al., 1997). Preliminary studies with human liver microsomes show activation by dapsone at low naproxen concentrations. The addition of 100 μM dapsone results in a hyperbolic naproxen saturation curve (data not shown). These results suggest that the metabolism of multiple NSAIDs is activated by dapsone.

DISCUSSION

The need to metabolize hydrophobic foreign compounds presents nature with a unique challenge. The vast array of xenobiotics makes it impractical to have one enzyme for each compound or even each class of compounds. Therefore, while most cellular functions tend to be very specific, xenobiotic metabolism requires enzymes with diverse substrate specificities. The cytochrome P450s have apparently assumed much of this role. The required diversity is accomplished by families and subfamilies of enzymes with generally broad substrate specificities and a very reactive oxygenating species. Therefore, while the relatively small number of cytochrome P450s associated with the oxidation of endogenous substrates, i.e., steroidogenesis (Jefcoate, 1986) and prostaglandin metabolism (Masters et al., 1987), tend to be highly restrictive in their substrate specificities, the xenobiotic-metabolizing P450s have broad substrate selectivities and regioselectivities (multiple sites of oxidation).

Broad substrate specificities are most likely achieved through relatively nonspecific binding interactions. Since P450 substrates are hydrophobic, these binding interactions are probably hydrophobic in nature. Although steric restrictions may be an important determinant of the substrate selectivity of the P450 enzymes, many P450 enzymes can metabolize substrates of varying sizes. The combination of relatively nonspecific binding interactions and lenient size requirements suggests that multiple molecules might bind in a P450 active site. For example, many of the P450 enzymes can metabolize polycyclic aromatic hydrocarbons (PAHs)(Shou et al., 1994b). The size of the PAHs can vary from naphthalene (two aromatic rings) to very large substrates such as dibenzopyrenes (six rings). If an active site can accommodate very large substrates, it might be expected that more than one naphthalene molecule can be bound. Indeed, many of the P450 enzymes show non-Michaelis−Menten kinetics for naphthalene metabolism. Finally, it has been shown by NMR studies that both pyridine and imidazole can coexist in the P450cam active site (Banci et al., 1994). Thus, even a P450 with relatively rigid structural requirements can simultaneously bind two small substrates.

Based on the crystal structures of bacterial enzymes and sequence alignments of mammalian enzymes, it is generally accepted that the P450 enzymes contain only one active site. We use the model in Figure 1 to represent the multiple substrates binding to a P450 active site. In our model, the relative orientation of the substrates is not defined. However, two extremes can be envisioned: (1) each substrate occupies a distinct and defined area within the active site; (2) although

each substrate must occupy different regions of the active site at any one time, there is no particular orientation of either substrate in the active site. In either case, both substrates must have access, through translations and rotations, to the reactive oxygen within the time frame of the substrate oxidation step. Isotope effect experiments have shown that substrate rotation rates within the active site are faster than the rate of the substrate oxidation step (Foster, 1985; Jones et al., 1986; Jones & Trager, 1987; Korzekwa et al., 1989, 1995). In these experiments, a decrease in metabolism at one position of a substrate due to deuterium substitution results in an increase in metabolism at another position. For this to occur, the rate of exchange between the two positions must be faster than the rate of hydrogen abstraction. Although the rate of rotation generally decreases as the size of the molecule increases (Iyer et al., 1997), rotation rates can be significant for some large substrates. For example, deuterium substitution in the 6β-position of testosterone results in a 3-fold increase in 15β-hydroxylation with expressed CYP3A4 (unpublished results). Thus, rapid reorientation within the active site provides the means for each substrate to have access to the active oxygen.

The experimental data presented above can be fit to the equations derived for the two-substrate models. However, these models and equations do not distinguish between two substrates binding in the same active site or the presence of multiple independent binding sites. When only one substrate is used, the nature of the interaction cannot be determined. For substrate inhibition and autoactivation (sigmoidal saturation curves), the second substrate could be interacting at completely independent sites, even different proteins, e.g., P450 reductase. However, when a second molecule is used as an effector (activator or inhibitor) and the second molecule is also a substrate, the nature of the second binding site can be evaluated.

If an effector molecule is also a substrate, then it must bind to the P450 active site (i.e., have access to the active oxygen). If a second binding site is also present on the enzyme, then inhibition could occur as a result of effector binding at either of the two sites. However, activation must occur by binding to a site that does not result in substrate displacement. Possibilities include either an allosteric site or the simultaneous binding into the same active site. If activation occurs when the effector binds to an independent allosteric site, then the substrate must be capable of inhibiting the metabolism of the effector by displacing it from the active site. The data on the interactions between phenanthrene and 7,8-benzoflavone (Table 1, and Figures 12 and 13) clearly show that phenanthrene cannot displace 7,8-benzoflavone from the active site and 7,8-benzoflavone cannot displace phenanthrene from the active site. The data are also internally consistent with similar K_m and K_B values when the compounds act as either substrate or effector ($K_m = 31$ μM and $K_B = 29$ μM for phenanthrene, and $K_m = 40$ μM and $K_B = 49$ μM for 7,8-benzoflavone).

A series of reactions showing non-Michaelis−Menten kinetics for the CYP3A enzymes were described by Ueng et al. (1997). For most of these reactions, 7,8-benzoflavone either activated or inhibited the reactions. In some cases, 7,8-benzoflavone activated at low substrate concentrations and inhibited at high substrate concentrations. The presence of 7,8-benzoflavone usually resulted in more hyperbolic reaction kinetics, suggesting that 7,8-benzoflavone prevented a second substrate molecule from binding. These results can be explained by the presence of an independent, allosteric binding site. However, it was also reported that 7,8-benzoflavone activates aflatoxin B_1, and aflatoxin B_1 does not inhibit 7,8-benzoflavone metabolism (Ueng et al., 1997). Again, these results suggest that both substrates have access to the reactive oxygen; i.e., both molecules are present in the same active site. Recently, partial inhibition kinetics were reported for the interaction between testosterone and erythromycin with CYP3A4 (Wang et al., 1997). Since neither substrate could completely inhibit the metabolism of the other, a two site model in which both substrates have access to the active oxygen was proposed.

The data in Table 2 suggest that neither phenanthrene nor 7,8-benzoflavone alters each others binding characteristics. As mentioned in our previous report (Shou et al., 1994a), the lack of a change in K_m for the phenanthrene−7,8-benzoflavone interaction may be due to the small size of phenanthrene and is probably the exception, rather than the rule. Often, 7,8-benzoflavone and other activators alter the regioselectivity of the P450 oxidations (Imaoka et al., 1992; O'Shaughnessy & Mannan, 1994; Ueng et al., 1995, 1997). The ability of many P450 enzymes to oxidize a substrate in more than one position suggests that the orientation of the substrate in the active site is not well-defined. Although the observed changes in regioselectivities could be due to conformational changes in the enzyme, they are also consistent with multiple substrates in an enzyme active site. The changes in regioselectivities are not random, but tend to show a shift toward metabolism of the narrower portion of the substrate molecules (Imaoka et al., 1992; O'Shaughnessy & Mannan, 1994; Ueng et al., 1995, 1997). This suggests that additional steric constraints have been made at the P450 active site.

Although originally used to describe ligand binding, the term "cooperativity" is often used to describe most non-Michaelis−Menten kinetics. Neet has suggested that the term be used in a phenomenological sense to describe all non-Michaelis−Menten kinetics with the exception of substrate inhibition (Neet, 1980). The above analyses show that two-substrate models can be used to describe most atypical cytochrome P450 kinetics, including substrate inhibition. However, other equations can provide good fits to experimental data. The analyses of Ueng et al. (1997) and the data in Table 1 show that good fits to to some experimental data sets can be obtained with the Hill equation. In addition to hyperbolic and sigmoidal saturation curves, the Hill equation will also fit the biphasic saturation curves (Figures 3G, 9, and 11) with $n < 1$. However, neither the binding constant nor the exponent for the Hill equation have any direct relationship to K_m and V_{max} values. In fact, the interpretation of $n<1$ for biphasic saturation curves (Figures 3G, 9, and 11) would suggest negative cooperativity, whereas the velocity of the reaction is increased by the binding of a second substrate. Finally, the Hill equation does not provide good fits to substrate inhibition curves.

Unfortunately, as shown in Figure 2 and Table 1, there is no unique solution to eq 1 for sigmoidal saturation curves. The sigmoidal curve can be due either to $K_{m2} < K_{m1}$ or to $V_{max2} > V_{max1}$, or a combination of the two. Therefore, without additional data, the correct values of the kinetic

parameters cannot be determined. Multiple-substrate studies can provide additional information about the values of the kinetic parameters. For example, two solutions to the dapsone saturation curve (Figure 10 and Table 1) are: (1) $V_{max1} = 0.02$, $V_{max2} = 0.58$ μM, $K_{m1} = 10$ μM, $K_{m2} = 110$; and (2) $V_{max1} = V_{max2} = 0.48$, $K_{m1} = 262$ μM, $K_{m2} = 53$ μM. However, the fit of the data in Figure 14 to eq 4 gives a dapsone binding constant of 17 μM. Therefore, it is likely that the sigmoidal saturation curve for dapsone metabolism is due to $V_{max2} > V_{max1}$.

It should be noted that the detailed kinetics for the cytochrome P450 enzymes are likely to be more complicated than are described by our simple models. For example, Friedman et al. have shown by CO diffusion studies that multiple P450 conformations are likely to be present in the microsomal membrane (Koley et al., 1994, 1995a,b, 1997a,b). The authors suggest that activation of benzo[*a*]pyrene (BaP) metabolism CYP3A4 by 7,8-benzoflavone is due to an allosteric interaction that converts a conformation that cannot metabolize BaP into one that can (Koley et al., 1997a). However, the authors model does not consider that 7,8-benzoflavone is also a substrate for CYP3A4. If a similar mechanism is invoked for the activation of phenanthrene metabolism by CYP3A4, it would require that one conformation that cannot bind 7,8-benzoflavone in the active site metabolizes phenanthrene and a second conformation that cannot bind phenanthrene in the active site metabolizes 7,8-benzoflavone. Although this and other more complicated mechanisms cannot be excluded with the present experimental data, the models and equations presented can adequately describe non-Michaelis−Menten P450 kinetics.

In summary, two-substrate models can be used to describe activation, autoactivation, partial inhibition, substrate inhibition, and biphasic saturation curves for the cytochrome P450 enzymes. When an effector is also a substrate, the inability of the substrate to displace the effector from the active site, and vice versa, suggests that both compounds are bound simultaneously to the P450 active site. Although atypical kinetics are most common for the CYP3A enzymes, they can be observed for other P450 enzymes as well.

REFERENCES

Banci, L., Bertini, I., Marconi, S., Pierattelli, R., & Sligar, S. G. (1994) *J. Am. Chem. Soc. 116*, 4866.

Cleland, W. W. (1979) *Methods Enzymol. 63*, 500.

Coleman, M. D., Breckenridge, A. M., & Park, B. K. (1989) *Br. J. Clin. Pharmacol. 28*, 389.

Foster, A. B. (1985) *Adv. Drug Res. 14*, 1.

Gonzalez, F. J., Aoyama, T., & Gelboin, H. V. (1991) *Methods Enzymol. 206*, 85.

Haining, R. L., Hunter, A. P., Veronese, M. E., Trager, W. F., & Rettie, A. E. (1996) *Arch. Biochem. Biophys. 333*, 447.

Imaoka, S., Imai, Y., Shimada, T., & Funae, Y. (1992) *Biochemistry 31*, 6063.

Iyer, K. R., Jones, J. P., Darbyshire, J. F., & Trager, W. F. (1997) *Biochemistry 36*, 7136.

Jefcoate, C. (1986) in *Cytochrome P-450* (Ortiz de Montellano, P. R., Ed.) pp 387−428, Plenum Press, New York.

Johnson, E. F., Schwab, G. E., & Vickery, L. E. (1988) *J. Biol. Chem. 263*, 17672.

Jones, J. P., & Trager, W. F. (1987) *J. Am. Chem. Soc. 109*, 2171.

Jones, J. P., Korzekwa, K. R., Rettie, A. E., & Trager, W. F. (1986) *J. Am. Chem. Soc. 108*, 7074.

King, E. L., & Altman, C. (1956) *J. Chem. Phys. 60*, 1375.

Koley, A. P., Robinson, R. C., Markowitz, A., & Friedman, F. K. (1994) *Biochemistry 33*, 2484.

Koley, A. P., Buters, J. T. M., Robinson, R. C., Markowitz, A., & Friedman, F. K. (1995a) *J. Biol. Chem. 270*, 5014.

Koley, A. P., Robinson, R. C., Markowitz, A., & Friedman, F. K. (1995b) *Biochemistry 34*, 1942.

Koley, A. P., Buters, J. T. M., Robinson, R. C., Markowitz, A., & Friedman, F. K. (1997a) *J. Biol. Chem. 272*, 3149.

Koley, A. P., Robinson, R. C., Markowitz, A., & Friedman, F. K. (1997b) *Biochem. Pharmacol. 53*, 455.

Korzekwa, K. R., Trager, W. F., & Gillette, J. R. (1989) *Biochemistry 28*, 9012.

Korzekwa, K. R., Trager, W. F., & Gillette, J. R. (1995) *Drug Metab. Rev. 27*, 45.

Masters, B. S. S., Muerhoff, A. S., & Okita, R. T. (1987) in *Mammalian Cytochromes P-450* (Guengerich, F. P., Ed.) pp 107−131, CRC Press, Boca Raton.

May, D. G., Arns, P. A., Richards, W. O., Porter, J., Ryer, D., Fleming, C. M., Wilkinson, G. R., & Branch, R. A. (1992) *Clin. Pharmacol. Ther. 51*, 689.

Neet, K. E. (1980) *Methods Enzymol. 64*, 139.

Omura, T., & Sato, R. (1964) *J. Biol. Chem. 239*, 2370.

O'Shaughnessy, P. J., & Mannan, M. A. (1994) *Mol. Cell. Endocrinol. 104*, 133.

Schwab, G. E., Raucy, J. L., & Johnson, E. F. (1988) *Mol. Pharmacol. 33*, 493.

Segel, I. H. (1975) in *Enzyme Kinetics*, John Wiley & Sons, Inc., New York.

Shou, M., Grogan, J., Mancewicz, J. A., Krausz, K. W., Gonzalez, F. J., Gelboin, H. V., & Korzekwa, K. R. (1994a) *Biochemistry 33*, 6450.

Shou, M., Korzekwa, K. R., Krausz, K. W., Crespi, C. L., Gonzalez, F. J., & Gelboin, H. V. (1994b) *Cancer Lett. 83*, 305.

Tracy, T. S., Marra, C., Wrighton, S. A., Gonzalez, F. J., & Korzekwa, K. R. (1996) *Biochem. Pharmacol. 52*, 1305.

Tracy, T. S., Marra, C., Wrighton, S. A., Gonzalez, F. J., & Korzekwa, K. R. (1997) *Eur. J. Clin. Pharmacol.* (in press).

Ueng, Y., Kuwabara, T., Chun, Y., & Guengerich, F. P. (1997) *Biochemistry 36*, 370.

Ueng, Y.-F., Shimada, T., Yamazaki, H., & Guengerich, F. P. (1995) *Chem. Res. Toxicol. 8*, 218.

Wang, R. W., Newton, D. J., Scheri, T. D., & Lu, A. Y. H. (1997) *Drug Metab. Dispos. 25*, 502.

Wrighton, S. A., Maurel, P., Scheutz, E. G., Watkins, P. B., Young, B., & Guzelian, P. S. (1985) *Biochemistry 24*, 2171.

BI9715627